



# Active stabilization of alkali-atom vapor density with a solid-state electrochemical alkali-atom source

SONGBAI KANG,<sup>1,\*</sup> RUSSELL P. MOTT,<sup>2</sup> ALLISON V. MIS,<sup>2,3</sup> CHRISTOPHER S. ROPER,<sup>2</sup> ELIZABETH A. DONLEY,<sup>1</sup> AND JOHN KITCHING<sup>1</sup>

<sup>1</sup>NIST, 325 Broadway, Boulder, Colorado 80305, USA

<sup>2</sup>HRL Laboratories, LLC, Malibu, California 90265, USA

<sup>3</sup>Current address: Colorado School of Mines; Golden, CO 80401, USA

\*songbai.kang@nist.gov

**Abstract:** We report a demonstration of vapor-phase Rubidium (Rb) density stabilization in a vapor cell using a solid-state electrochemical Rb source device. Clear Rb density stabilization is observed. Further demonstrations show that the temperature coefficient for Rb density can be reduced more than 100 times when locked and the device's power consumption is less than 10 mW. Preliminary investigation of the locking dynamic range shows that the Rb density is well stabilized when the initial density is five times higher ( $33 \times 10^9 / \text{cm}^3$ ) than the set point density ( $6 \times 10^9 / \text{cm}^3$ ). Active stabilization with this device is of high interest for portable cold-atom microsystems where large ambient temperature working ranges and low power consumption are required.

© 2018 Optical Society of America under the terms of the [OSA Open Access Publishing Agreement](#)

**OCIS codes:** (020.0020) Atomic and molecular physics; (120.3930) Metrological instrumentation; (300.6320) Spectroscopy, high-resolution; (130.6010) Sensors.

## References and links

1. J. Guéna, P. Rosenbusch, P. Laurent, M. Abgrall, D. Rovera, G. Santarelli, M. E. Tobar, S. Bize, and A. Clairon, "Demonstration of a dual alkali Rb/Cs fountain clock," *IEEE Trans. Ultrason. Ferroelectr. Freq. Control* **57**(3), 647–653 (2010).
2. D. S. Durfee, Y. K. Shaham, and M. A. Kasevich, "Long-term stability of an area-reversible atom-interferometer Sagnac gyroscope," *Phys. Rev. Lett.* **97**(24), 240801 (2006).
3. H. Müller, S. W. Chiow, S. Herrmann, S. Chu, and K. Y. Chung, "Atom-interferometry tests of the isotropy of post-Newtonian gravity," *Phys. Rev. Lett.* **100**(3), 031101 (2008).
4. B. Battelier, B. Barrett, L. Fouché, L. Chiechet, L. Antoni-Micollier, H. Porte, F. Napolitano, J. Lautier, A. Landragin, and P. Bouyer, "Development of compact cold-atom sensors for inertial navigation," *Proc. SPIE* **9900**, 990004 (2016).
5. C. Monroe, W. Swann, H. Robinson, and C. Wieman, "Very cold trapped atoms in a vapor cell," *Phys. Rev. Lett.* **65**(13), 1571–1574 (1990).
6. B. P. Anderson and M. A. Kasevich, "Loading a vapor-cell magneto-optic trap using light-induced atom desorption," *Phys. Rev. A* **63**(2), 023404 (2001).
7. T. Karaulanov, M. T. Graf, D. English, S. M. Rochester, Y. J. Rosen, K. Tsigutkin, D. Budker, E. B. Alexandrov, M. V. Balabas, D. F. J. Kimball, F. A. Narducci, S. Pustelny, and V. V. Yashchuk, "Controlling atomic vapor density in paraffin-coated cells using light-induced atomic desorption," *Phys. Rev. A* **79**(1), 012902 (2009).
8. S. Villalba, H. Failache, and A. Lezama, "Light-induced atomic desorption and diffusion of Rb from porous alumina," *Phys. Rev. A* **81**(3), 032901 (2010).
9. P. F. Griffin, K. J. Weatherill, and C. S. Adams, "Fast switching of alkali atom dispensers using laser-induced heating," *Rev. Sci. Instrum.* **76**(9), 093102 (2005).
10. V. Dugrain, P. Rosenbusch, and J. Reichel, "Alkali vapor pressure modulation on the 100 ms scale in a single-cell vacuum system for cold atom experiments," *Rev. Sci. Instrum.* **85**(8), 083112 (2014).
11. M. Stephens, R. Rhodes, and C. Wieman, "Study of wall coatings for vapor-cell laser traps," *J. Appl. Phys.* **76**(6), 3479–3488 (1994).
12. S. Kang, R. P. Mott, K. A. Gilmore, L. D. Sorenson, M. T. Rakher, E. A. Donley, J. Kitching, and C. S. Roper, "A low-power reversible alkali atom source," *Appl. Phys. Lett.* **110**(24), 244101 (2017).
13. S. Rochester, "Linear absorption fitting," version 2010.04.20, a package of AtomicDensityMatrix open source software, 2017. <http://rochesterscientific.com/ADM/#documentation>.

14. A. Klein, O. Witzel, and V. Ebert, "Rapid, time-division multiplexed, direct absorption- and wavelength modulation-spectroscopy," *Sensors (Basel)* **14**(11), 21497–21513 (2014).

## 1. Introduction

Atomic clocks and sensors based on laser-cooled atom technology have already shown outstanding performance with respect to those based on room temperature vapors, especially in terms of long-term stability and accuracy [1–4]. However most of these cold-atom systems must be operated in a controlled laboratory environment and are not well suited to portable applications, particularly because keeping a constant alkali-atom density in a vapor cell is a significant challenge outside the laboratory. The characteristics of the magneto-optical trap (MOT) (e.g. loading rate, loss rate, and cooling beam intensity) are greatly dependent on the background alkali-atom density, so large variations in environment temperature degrade the performance of atom clocks and sensors [5], and may even destroy MOT trapping. In addition, too high an alkali-atom background pressure will create excessive background fluorescence which makes the detection of the cold atoms very difficult. Some techniques such as light induced atom desorption (LIAD) [6–8] and thermally activated alkali sources (either induced by a laser or current [9,10]) have demonstrated that they can efficiently modulate alkali-atom partial pressures in a vapor cell in a laboratory environment, but there are few investigations about how well the density can be stabilized when the environment temperature changes. Alkali atom adsorption rates depend on the temperature and the geometry of the vapor cell; changes in the temperature lead to changes in the adsorption and desorption rates of alkali atoms that unintentionally modulate the atom density [11]. Moreover, these previous techniques can only precisely modulate alkali-atom pressure after the curing phenomenon finishes in the cell [11]. Furthermore, while temperature stabilization of the vapor cell is an effective method for stabilizing density, it consumes considerable power, especially for cooling.

## 2. Experimental setup

In this letter, we demonstrate active stabilization of Rb vapor-phase density with a solid-state electrochemical Rb source. The device consists of a solid ion conductor (Sodium-beta" -alumina: Na-  $\beta$ " -alumina) sandwiched between two electrodes. The device can both sink and source Rb when an appropriately polarized voltage is applied across the electrodes [12]. Figure 1 depicts a schematic of the experimental setup. The whole vacuum system consists of a vapor cell, two Na-  $\beta$ " -alumina devices (each about 3 cm  $\times$  1 cm), a Rb commercial dispenser, a turbo pump, and a residual gas analyzer (RGA). The RGA was used to monitor contaminant gases and ensure that the device was completely degassed before collecting Rb vapor pressure measurements. A base pressure of  $10^{-7}$  Torr was achieved after baking the vacuum system at 100 °C.

A 795 nm laser beam travels between the two Na-  $\beta$ " -alumina devices and is then detected by a photo detector (PD). The PD output is split into two paths: one is for detecting the direct absorption spectrum and is used to calibrate the Rb vapor density by fitting the direct linear absorption spectrum [13], while the other is for second harmonic frequency modulation (FM) spectroscopy [14]. Saturated absorption spectroscopy (SAS) locking and a noise eater are used to suppress the laser's frequency and intensity drifts.

During operation, electrical current is passed through the commercial Rb dispenser to load Rb into the cell. The signal to noise ratio (SNR) from the FM spectrum is about 100 times higher than that from the direct absorption, so the FM spectrum's amplitude value is fed into a proportional-integral (PI) servo to electrically control the voltage applied to the Na-  $\beta$ " -alumina devices. This servo voltage determines the degree to which the devices either source or sink Rb atoms to control Rb vapor density.

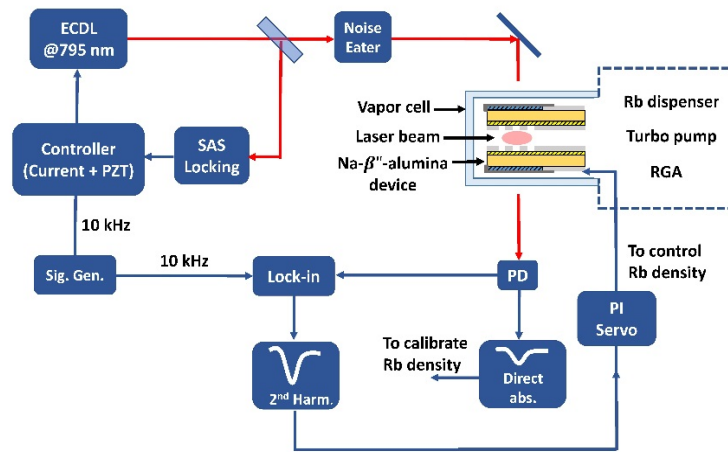


Fig. 1. Schematic of experimental setup for stabilizing the Rb density in an atomic vapor cell. Red beams indicate the laser, while blue beams indicate electronic signals. The dotted line indicates components connected to the vapor cell.

### 3. Experimental results

To demonstrate Rb density stabilization, we first apply a current through the Rb dispenser to achieve a Rb density baseline before switching on the servo to activate the source/sink abilities of the Na- $\beta''$ -alumina devices. Figure 2(a) shows that the Rb density drifts during the first 1250 s without servo stabilization. This is attributed to fluctuations in the cell temperature and/or the operating current of the Rb source. After switching on the servo, the Rb density is regulated to the set point after an initial transient period of 30 seconds, then kept stable at the set point for the following 1500 s. The Allan deviation of the density traces in Fig. 2(b) shows more than one order of magnitude improvement in the stability for times greater than 100 s when density is locked.

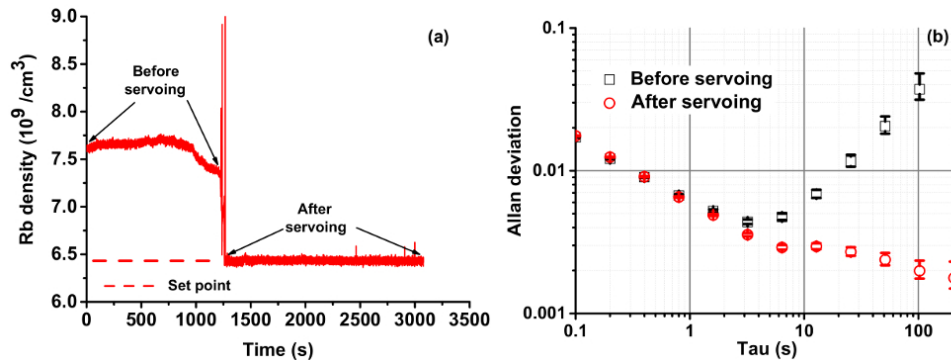


Fig. 2. Demonstration of Rb vapor density stabilization in a cell: (a) real time Rb density behavior before and after servoing; the initial density jump observed after engaging the servo results from non-ideal PI gain settings. (b) Allan deviation of the density fluctuation for the free running (black squares) and locked (red circles) period; the cell was not temperature stabilized.

To further investigate how well the servo system can stabilize the Rb density, we alternated the current through the Rb dispenser between 7.0 A and 6.7 A with a period of around 200 s and then compared the Rb density behavior before and after locking. In Fig. 3, the first two current pulses induce corresponding periodic Rb density drift whose amplitude is  $1.5 \times 10^9 / \text{cm}^3$ . The initial value of the current at  $t = 0$  was equal to the “high” value.

However, after locking, the Rb density drift is suppressed and tightly maintained at the set point. The inset of Fig. 3 shows transient Rb density bumps (made more obvious by adjacent averaging) when the current pulses are initially applied; however, the density is quickly regulated back to the set point. The Rb density drift amplitude when in the steady state is less than  $1 \times 10^7 / \text{cm}^3$  which means the Rb density temperature coefficient could be reduced 100 times when the system is locked. We note that the mean value of the current across each device when locking is only  $\sim 10 \mu\text{A}$  corresponding to a reduction in the number of Rb atoms of  $10^{14} / \text{s}$ , while the root mean square (RMS) of the current is  $\sim 500 \mu\text{A}$ . The feedback voltage on each device is around 10 V, so each device's power consumption to stabilize the Rb density in the cm-scale vapor cell is less than 10 mW. For comparison with heating-based density control, maintaining a cubic cell of volume  $1 \text{ cm}^3$  and emissivity of 1 at  $30 \text{ }^\circ\text{C}$  in an ambient temperature of  $-40 \text{ }^\circ\text{C}$  would take 200 mW to compensate for blackbody radiation alone. This represents significant power reduction and would be compatible with future portable battery-powered applications.

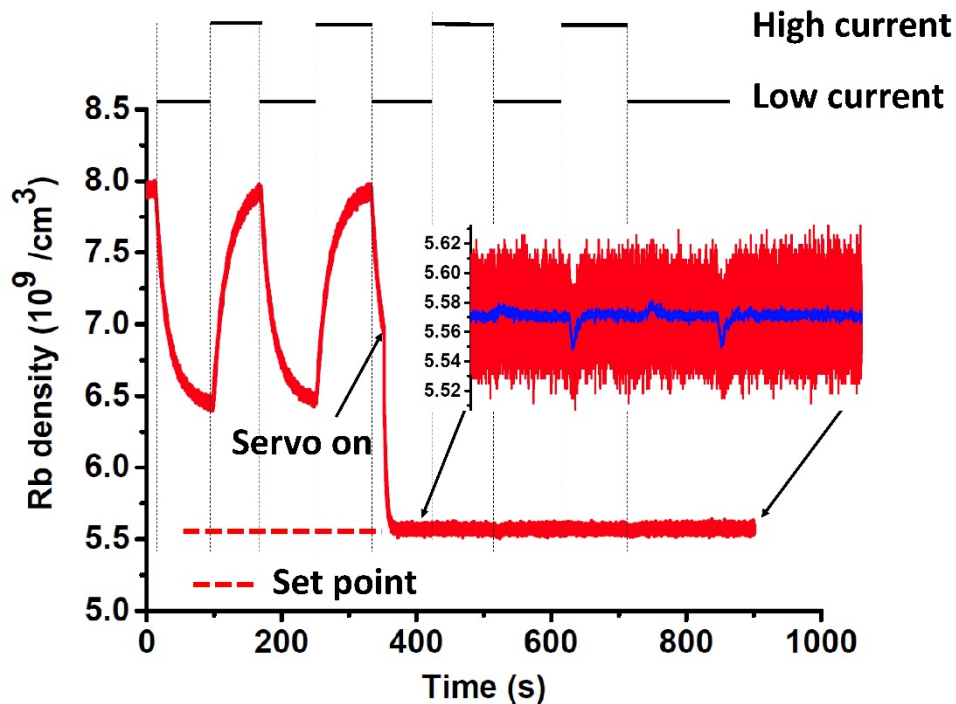


Fig. 3. Demonstration of Rb density stabilization when the current through the Rb dispenser is running in a pulsed mode (high current: 7.0 A; low current: 6.7 A). Inset: zoom in of data from 400 s to 900 s (red curve) and 100 times adjacent average (blue curve). The small bumps in the blue trace show a roughly 10 s locked system's response period due to sudden sharp changes in Rb density.

Effective servo systems perform well in both stability performance and locking dynamic range. Figure 4 displays preliminary test results for the locking range. Several Rb density responses are generated using different constant current values through the Rb dispenser before locking ( $t = 0 \text{ s}$  is the servo switch-on point). After switching on the servo, there are three different dynamic behaviors. For relatively low initial Rb densities ( $6.5 \times 10^9 / \text{cm}^3$  to  $7.5 \times 10^9 / \text{cm}^3$ ), the density is normally locked to the set point of  $6.2 \times 10^9 / \text{cm}^3$  within 10 s and then maintained. For medium initial Rb densities ( $\sim 10 \times 10^9 / \text{cm}^3$ ), oscillations are observed over  $\sim 15 \text{ s}$ , which then stabilize. The settings for the initial PI servo are fixed during the above tests. For high initial density level ( $33 \times 10^9 / \text{cm}^3$ ), the Rb density does not

settle to the set point after 13 s; to compensate for the nonlinear behavior, the servo P and I gain were adjusted around 15 s and the density was then successfully regulated to the set point after an additional 10 s. The test results show that the system can successfully stabilize the Rb density even when the initial density is  $30 \times 10^9 / \text{cm}^3$  above the set point level ( $6 \times 10^9 / \text{cm}^3$ ), this demonstrates a five-fold reduction in the Rb density. Improved stabilization at higher densities may be possible with different control loop tuning parameters.

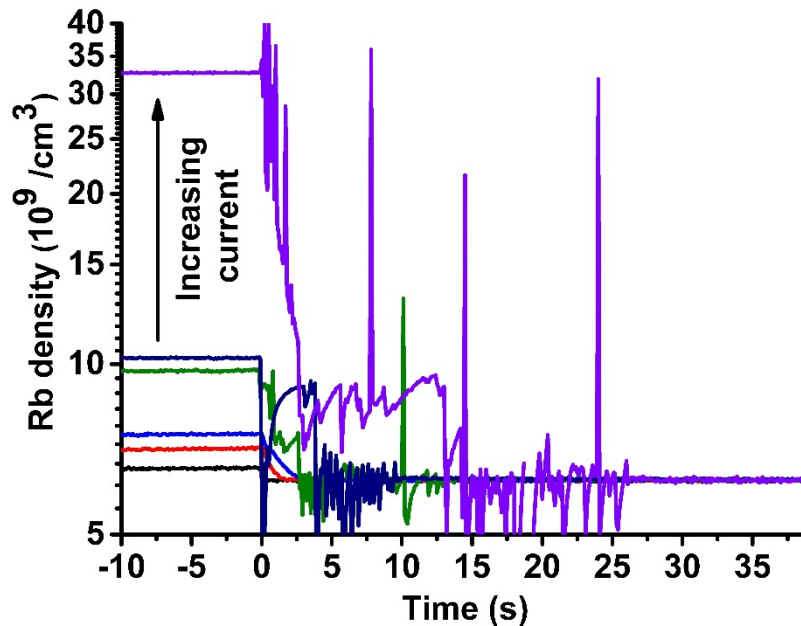


Fig. 4. Servo system locking behaviors under different currents through the SEAS dispenser.

#### 4. Conclusions

We demonstrate active stabilization of the Rb vapor density in a vapor cell using a solid-state electrochemical Rb source (Sodium-beta"-alumina). The time to achieve lock is  $\sim 10$  s but depends on the details of the servo implementation. Large swings in the Rb vapor density can be reduced by a factor of over 100. Moreover, the Rb density has been shown to be regulated to a set point of  $6 \times 10^9 / \text{cm}^3$  when the background density is sourced to an unregulated steady-state value of more than  $30 \times 10^9 / \text{cm}^3$ . A faster locking period and higher dynamic range are likely possible with further optimization of the electrochemical device. Further experiments will be continued in order to explore applications of this technology for laser-cooled Rb atoms and this core technology could translate to other alkali and alkaline earth elements that find a wide range of uses in cold-atom systems that need to work over large ambient temperature ranges. Additionally, these devices can be attractive for hot-vapor atomic clocks and sensors (e.g. NMR gyroscopes and magnetometers) to further stabilize alkali-atom density in combination with traditional cell temperature stabilization methods. Finally, the low power consumption of 10 mW for the alkali-atom vapor density locking can find suitable applications in miniature or micro atomic systems.

#### Funding

Defense Advanced Research Projects Agency (DARPA) and Space and Naval Warfare Systems Center Pacific (SSC Pacific) (Contract No. N66001-15-C-4027).

## Acknowledgments

The authors acknowledge DARPA program manager Robert Lutwak as well as Logan Sorenson, Matthew Rakher, Jason Graetz, John Vajo, Adam Gross, and Danny Kim of HRL Laboratories, LLC for useful discussions. We further acknowledge Florian Herrault, Giovanni Candia, Stephen Lam, Tracy Boden, Margie Cline, Ryan Freeman, and Lian-Xin Coco Huang for assistance with device fabrication. This work is a contribution of NIST, an agency of the U.S. government, and is not subject to copyright.